EUROPEAN FUSION DEVELOPMENT AGREEMENT

JET

EFDA–JET–CP(03)01-11

K. Crombé, Y. Andrew, I. Coffey, P. De Vries, C. Giroud, N.C. Hawkes, E. Joffrin,
D.C. McDonald, A. Murari, J. Ongena, F. Sattin, M. Valisa, K.D. Zastrow
and JET EFDA Contributors

Improved Measurements of Impurity Ion Poloidal Rotation Velocity in JET

Improved Measurements of Impurity Ion Poloidal Rotation Velocity in JET

K. Crombé[1], Y. Andrew[2], I. Coffey[2], P. De Vries[3], C. Giroud[3], N.C. Hawkes[2], E. Joffrin[5], D.C. McDonald[2], A. Murari[4], J. Ongena[6], F. Sattin[4], M. Valisa[4], K.D. Zastrow and JET EFDA Contributors*

[1]*Department of Applied Physics, Ghent University, Belgium*
[2]*Euratom/UKAEA Fusion Association, Culham Science Centre, Oxon, UK*
[3]*FOM-Rijnhuizen, ass. Euratom-FOM, TEC, PO Box 1027, 3430 BE Nieuwegein, NL*
[4]*Consorzio RFX-Associazione ENEA-Euratom per la fusione, Padova, Italy*
[5]*Ass.Euratom-CEA, Cadarache, FR*
[6]*LPP-ERM/KMS, Euratom-Belgian State Association, Trilateral Euregio Cluster, Belgium*
**See Annex of J. Pamela et al., "Overview of Recent JET Results and Future Perspectives", Fusion Energy 2000 (Proc. 18th Int. Conf. Sorrento, 2000), IAEA, Vienna (2001).*

Preprint of Paper to be submitted for publication in Proceedings of the EPS Conference on Controlled Fusion and Plasma Physics, (St. Petersburg, Russia, 7-11 July 2003)

INTRODUCTION

Both the toroidal and poloidal rotation velocities of ions are needed for the calculation of the total radial electric field, according to the formula:

$$E_r = \left(\frac{1}{Z_i en_i}\right)\left(\frac{dp_i}{dr}\right) - v_{\theta i} B_\varphi + v_{\varphi i} B_\theta, \tag{1}$$

where the first term is the contribution from the impurity pressure gradient and the second and third terms are the contributions from the poloidal ($v_{\theta i}$) and toroidal ($v_{\theta i}$) ion rotation velocities. Since the Er determines the E×B velocity and shear, the different contributions can influence the stabilization of turbulence and thus the formation of an Internal Transport Barrier (ITB). Of great interest are the mechanisms triggering the ITB formation, for example, a rapid change in poloidal velocity in a narrow radial layer has been observed in enhanced confinement regimes on other machines, as precursor for the barrier [1,2,3].

The toroidal rotation velocity and the impurity pressure profiles are measured on JET with Charge Exchange Recombination Rpectroscopy (CXRS). A second CXRS diagnostic is used for impurity poloidal rotation measurements. Since this diagnostic has both poloidal and toroidal components to the viewing chords, the poloidal velocity (v_θ) is derived from the Doppler shift of the spectral line ($\Delta\lambda/\lambda$), according to the formula:

$$\frac{\Delta\lambda}{\lambda} = -\frac{1}{c}(v_\theta \cos\theta + v_\varphi \cos\varphi), \tag{2}$$

where $\cos\theta$ and $\cos\phi$ are the cosine of the angle between the lines of sight and the poloidal and toroidal components of the magnetic field. Corrections to the apparent velocity due to the finite plasma temperature atomic effects are taken into account [6]. In previous analysis the values for $\cos\phi$ and $\cos\theta$ were calculated from the magnetic geometry, taking into account the design parameters of the diagnostic. It has been found that the largest error in the measurement of the poloidal rotation is introduced by the contribution of the toroidal rotation component ($v_\phi \cos\phi$) to the total line of sight velocity ($c\ \Delta\lambda/\lambda$) of this diagnostic [4]. In this paper we present results from dedicated experiments to improve the measurement technique. The idea was to allow a direct measurement of the toroidal rotation contribution, by keeping the poloidal rotation minimal and increasing the toroidal rotation during the discharge. We are able to estimate v_ϕ and $\cos\phi$, and using these results we show the temporal evolution of the poloidal rotation velocity in some ITB plasmas.

1. EXPERIMENT

A schematic view of the upper lines of sight (LOS) of the CXRS system used for the poloidal rotation measurement is shown in figure 1. The spatial resolution of the different channels varies from 4.5 cm for the outermost channels to ~10cm for the central viewing lines, depending on the magnetic geometry and the number of NBI PINIs that are used. The light is transmitted to a spectrometer, labelled as KS7, through fibre optics and six out of the fifteen fibre array are selected on a shot by shot basis, in order to avoid overlapping of the spectra on the CCD-camera. The temporal resolution for the measurements is 50ms. The *toroidal rotation* of the impurity ions is measured with a second CXRS system, consisting of 12 lines of sight almost parallel to the toroidal magnetic field at their intersections with the beams. The intersections are located between the plasma boundary and the plasma centre and provide a full radial profile. The light for this data is measured with the spectrometer labelled KS5a. Both CXRS diagnostics use Doppler shifted emission of the CVI charge exchange line at 529.1nm to determine the velocity profiles.

The main goal of the experiments was to determine the contribution of the toroidal velocity component to the total line of sight velocity of the poloidal rotation diagnostic. The plasmas were run with relatively high B_t (I_p / B_t = 2.5MA / 2.7T) to keep the L-mode for as long as possible, as can be seen from the divertor D-alpha trace in box 2 of figure 2, which shows no sign of a L-H transition. The NBI power was increased in steps during the pulse, as shown in box 1 of figure 2, to spin-up the toroidal rotation velocity. Box 5 shows the evolution in time of the toroidal rotation at 3.1m, the most central channel of the KS5 diagnostic and thus the highest measured toroidal velocity. We see a gradual increase, following the increasing beam power; a maximum value of about 140km/s is reached at 7MW NBI. A stepwise increase can be seen in the time evolution of the diamagnetic energy and the edge density following the increase in NBI power (boxes 3 and 4). To allow a direct measurement of the toroidal velocity component, the poloidal rotation during these L-mode plasmas, was kept low and constant [5]. In box 6 of figure 2 we have calculated the poloidal velocity using formula (2), the toroidal velocity from KS5 and the caculated values for $\cos\theta$ and $\cos\phi$. Although this calculation does not give an exact value for the poloidal velocity, we are able to check that the increase in NBI power during the discharge does not affect the poloidal rotation; the change in line of sight velocity is only due to a change in the toroidal component.

2. L-MODE SPIN-UP RESULTS

Since the viewing chords of both CXRS diagnostics look at different plasma radii, the first step in the analysis is the interpolation of the measured values of the toroidal velocity to the radial locations of the six channels of the poloidal CXRS diagnostic, to determine v_ϕ in formula (2). We use a cubic spline fit to the data and in figure 3 we show the measured values at the positions of the KS5 lines of sight, together with the interpolated values at the radial locations of the KS7 channels.

The next step is to determine the cosine of the angle between the lines of sight and the direction of the toroidal magnetic field, i.e. $\cos\phi$. In figures 4(a)-(b) we have plotted for two different channels of KS7, the total velocity along the lines of sight ($c\ \delta\lambda/\lambda$) as a function of the interpolated toroidal velocity (v_ϕ). It can be seen that a wide range of toroidal velocities is covered (from about 10 to 140 km/s). From fornula (2) and because of the constancy of the poloidal rotation with varying toroidal rotation as shown in the previous section, we can deduce from the slope of the linear fit in this plot a corrected value for $\cos\phi$, resulting from the experiment. The intersection of the linear fit with the

Y-axis, the second parameter determining the straight line, gives a measured value for ($v_\theta \cos\theta$). Since $\cos\theta$ is close to 1, this shows again that the poloidal velocity is low (<15 km/s for $\cos\theta = 0.95$). In table 1 themeasured and calculated values for $\cos\phi$ are compared for different channels of KS7 (from R = 3.41m to R = 3.65m). For these outer channels the calculated cosine underestimates the real value up to 18%. For the central channels (R<3.40m) the experimental data did not permit a good fit, but we extrapolated the results from the outer channels. Since the angle ϕ increases towards the central channels ($\phi > 77^o$ for R<3.40m), the contribution of the toroidal component becomes less important towards the central channels.

Table 1: Comparison of the measured and calculated values for cosφ

fibre radius	measured cosφ	calculated cosφ	difference
3.41 m	0.3727 +- 0.063	0.2334	0.1393 +- 0.063
3.47 m	0.4345 +- 0.048	0.2563	0.1782 +- 0.048
3.52 m	0.3559 +- 0.057	0.2779	0.078 +- 0.057
3.59 m	0.4669 +- 0.05	0.3014	0.1655 +- 0.05
3.65 m	0.3864 +- 0.06	0.3201	0.0663 +- 0.06
	extrapolated cosφ		
3.34m	0.3075 +- 0.05	0.206	0.1015 +- 0.05
3.29m	0.2884 +- 0.05	0.1828	0.1056 +- 0.05

3. POLOIDAL ROTATION IN ITB PLASMAS

Following the L-mode power scan experiments several plasmas were run with different heating schemes to create internal transport barriers. The time of formation of the barrier is determined from changes in the electron and ion temperature profiles and changes in the rate of increase of electron density and total neutron rate as shown by examples in figures 5(a-b).

In the first type of ITB plasmas, the barrier was created using 10MW of NBI, 5MW of ICRH and 1MW of LHCD as shown in figure 6a. From the ion temperature profile and total neutron rate, we see that the ITB initially formed at 5s as indicated in figure 5(a), and coincides with the main heating phase; a second and stronger barrier was formed at 6.5s. The ITBs are located at about 3.3m. The temporal evolution of the CVI poloidal rotation velocity, calculated using the measured values of the cosine angles, show a rapid change in the impurity poloidal velocity of 100km/s at 4.55s and of 60km/s at 4.75s at R=3.34m. The error on the poloidal velocity due to the uncertainty on $\cos\phi$, is between 5-10km/s, depending on the toroidal velocity. The sudden change corresponds to 450-250ms prior to the barrier formation and no such excursions in velocity were measured along the other lines of sight.

For the *second* series of ITB plasmas the barrier was created using 12MW of NBI and 6MW of ICRH. For both the plasmas shown in figure 6(b) the ITB is formed at about 5.5s, as indicated in the electron temperature profiles from the ECE measurements in figure 5(b) and is located around 3.4-3.5m. The ion temperature profile and total neutron rate increase somewhat later, at 5.7s. The CVI poloidal rotation had a large dip of 60km/s at around 5.15s at a radial location of 3.29m. No such change in poloidal rotation velocity was measured along the adjacent channels and the excursion in poloidal rotation precedes the ITB formation by 350ms. At 5.25s the poloidal velocities along the channels 3.34m and 3.41m start to diverge, this shear occurs 250ms before the onset of the barrier.

CONCLUSIONS

We have presented results from L-mode spin-up pulses to improve the calculation of the poloidal rotation velocity using Doppler shift measurements of charge exchange lines of impurities. These experiments have shown that the contribution of the toroidal rotation velocity component is important and needs to be corrected in the calculation.

In addition different ITB plasmas were analysed, taking into account the new cosine results. In the three different ITB plasmas studied, a localised change in the poloidal rotation velocity of 60km/s was seen about 300ms before the barrier formation.

REFERENCES

[1]. R.E. Bell et al., Phys. Rev. Lett. **81**, 1429 (1998)

[2]. S. de Peña Hempel et al., 25th EPS Conference, Prague (1998)

[3]. C.L. Rettig et al., 26th EPS Conference, Maastricht (1999)

[4]. F. Sattin et al., 28th EPS Conference, Madeira(2001)

[5]. N. Hawkes et al., Plasma Phys. Control. Fusion **38** (1996) 1261-1266

[6]. M. von Hellerman et al., Plasma Phys. Control. Fusion **37** (1995) 71-94

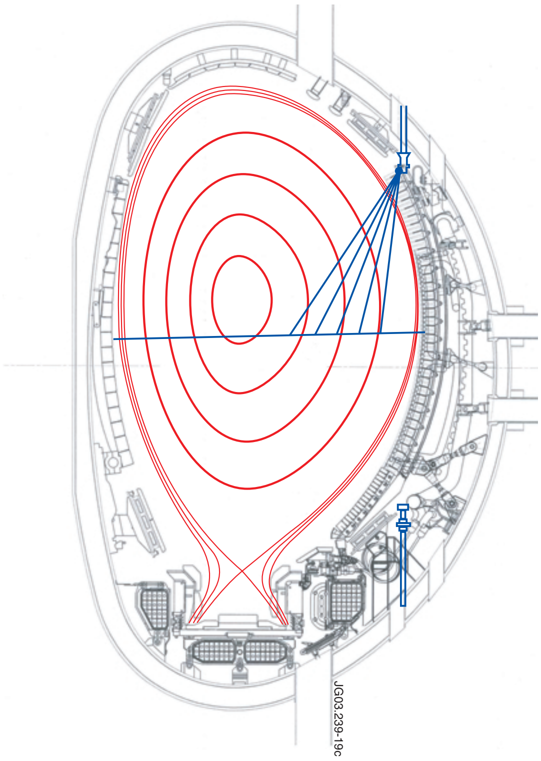

Figure 1: Setup of the CXRS diagnostic to measure poloidal rotation at JET (KS7).

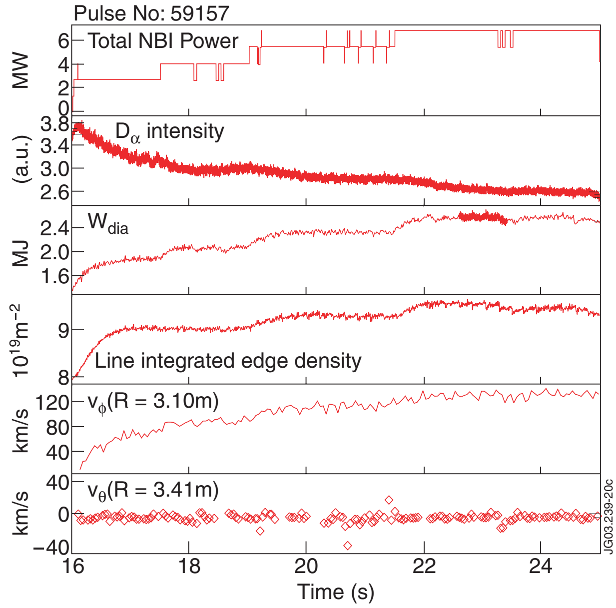

Figure 2: General parameters for the L-mode power scan experiments.

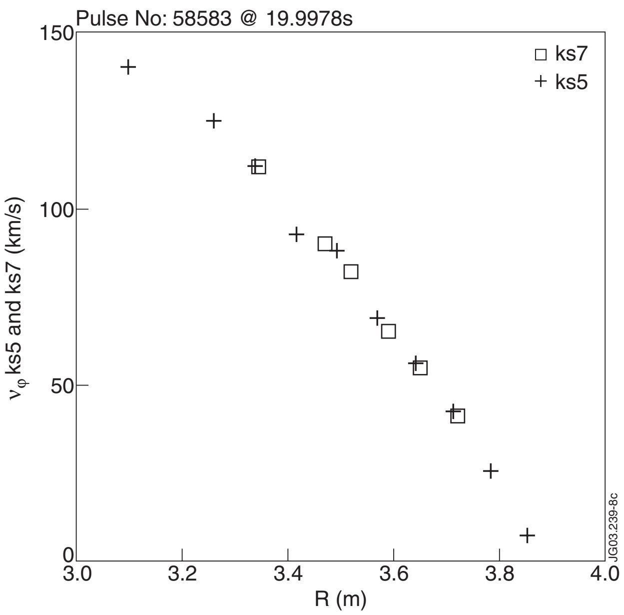

Figure 3: Interpolation of the KS5 toroidal rotation data to the KS7 lines of sight.

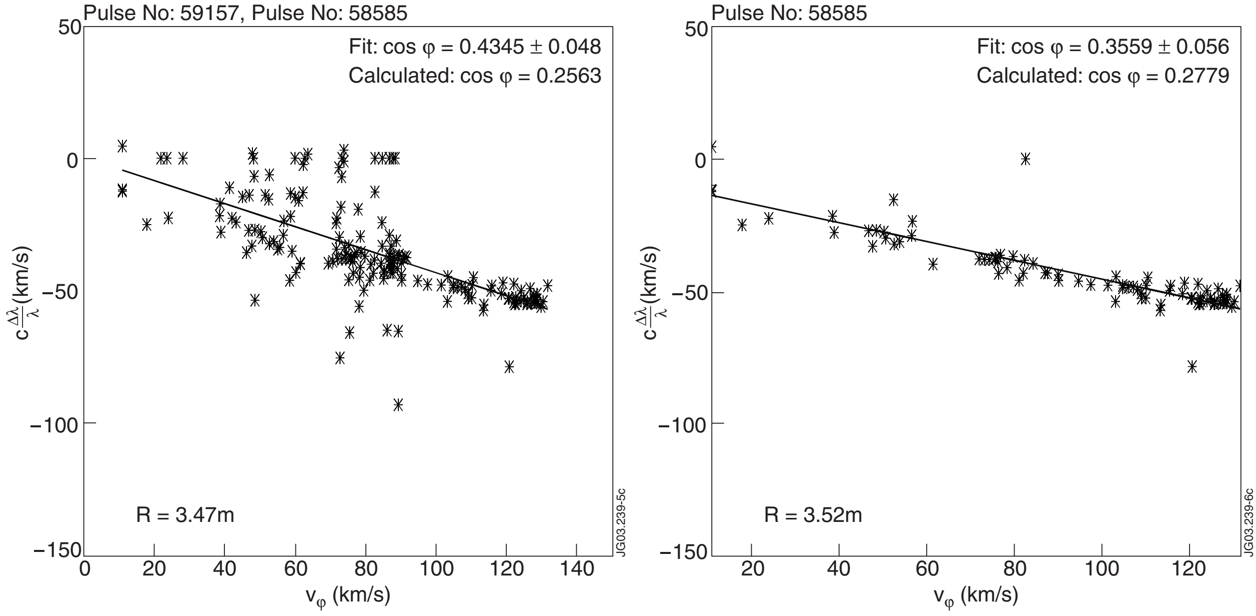

Figure 4(a-b): $c\,\dfrac{\Delta\lambda}{\lambda}$ versus v_φ for two different radial locations. Linear fit of the data points.

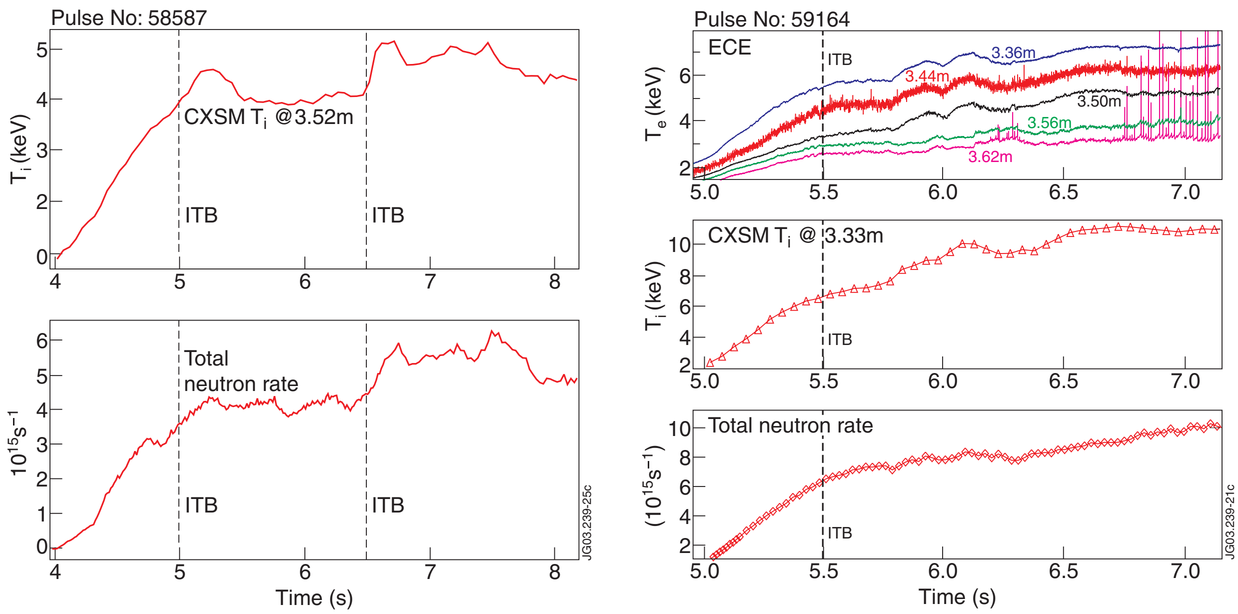

Figure 5(a-b): Determination of the time of ITB formation for two different pulses.

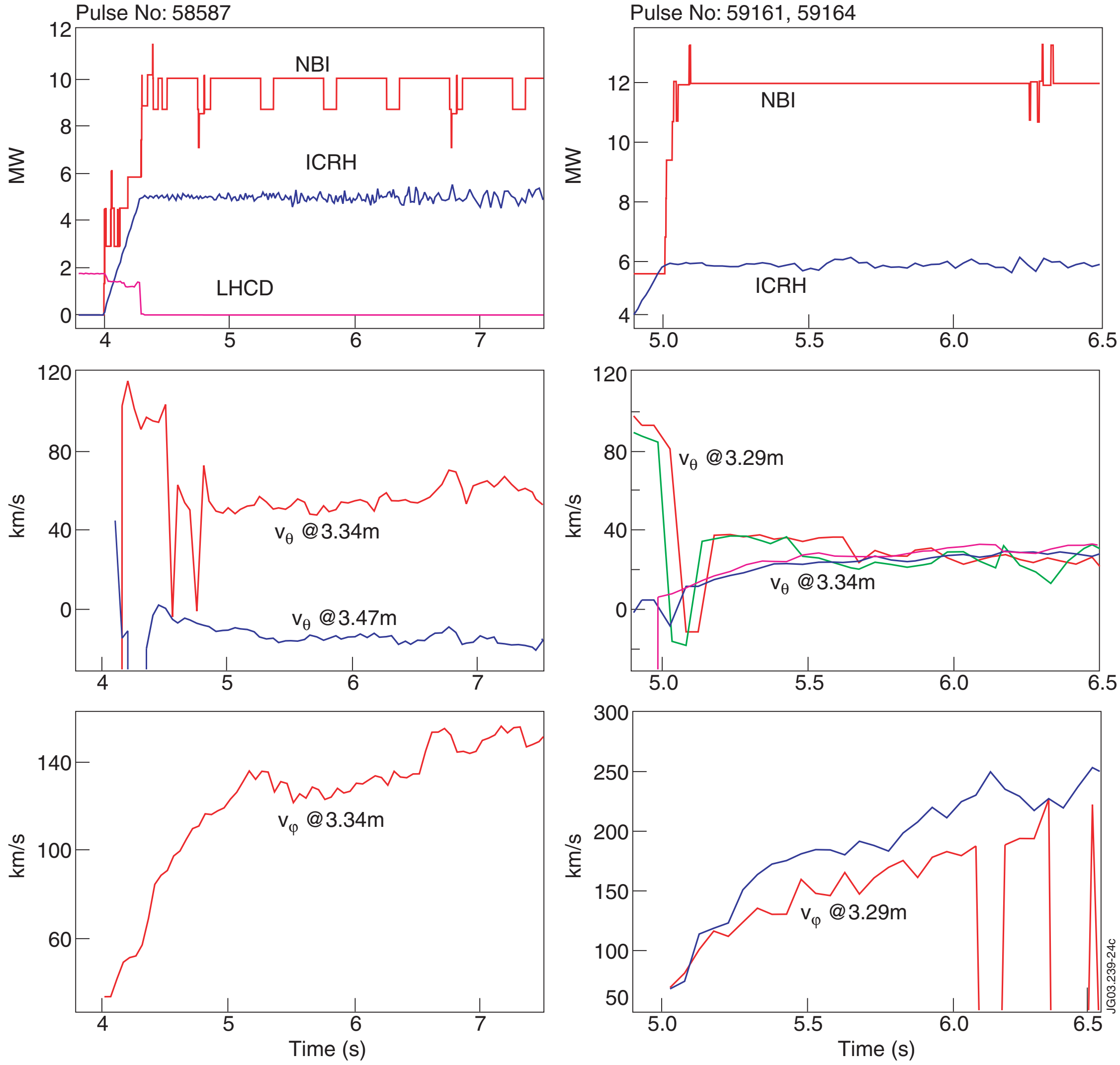

Figure 6: The heating scheme and poloidal and toroidal rotation for the two series of ITB plasmas